

# On the evolution of a stellar system in the context of the virial equation

V. Yu. Terebizh\*

Crimean Astrophysical Observatory

September 6, 2023

## Abstract

The virial equation is used to clarify the nature of the dynamic evolution of a stellar system. Compared to the kinetic equation, it gives a deeper but incomplete description of the process of relaxation to a quasi-stationary state, which here means the fulfillment of the virial theorem. Analysis shows that the time to reach the virial equilibrium state  $T_v$  is about two to three dozen dynamic time periods  $T_d$ . Namely, during  $T_v$  the virial ratio, the mean harmonic radius, and the root-mean-square radius of the system fluctuate, and then the first two characteristics stabilize near their equilibrium values, while the root-mean-square radius continues to grow (possibly ad infinitum). This indicates a fundamentally different behavior of the moment of inertia of the system relative to the center of gravity and its potential energy, leading to the formation of a relatively small equilibrium core and an extended halo.

Key words: Stellar dynamics (1596)

## 1 Introduction

Theoretical considerations, reinforced in recent years by extensive numerical simulations, show that the dynamical evolution of a stellar system in its own gravitational field is characterized by three basic time scales.

---

\*E-mail: valery@terebizh.ru

The shortest of them, the *dynamic time*  $T_d \sim (G\rho)^{-1/2}$ , where  $G$  is the gravitational constant and  $\rho$  – the mass-average density of the system, is associated with large-scale motions of matter in the early stages of system evolution. This parameter is also called the *crossing time*, because the return time of a body that has fallen from the surface of a homogeneous ball of density  $\rho$  into a hole passing along its diameter is equal to  $(3\pi/G\rho)^{1/2}$ .

According to Jeans (1915, 1919), the subsequent relaxation of the system to a quasi-stationary state in the smoothed, so-called *regular* gravitational field is described by the *collisionless Boltzmann equation* for the distribution function  $f(\mathbf{r}, \mathbf{v}, t)$  in 6-dimensional phase space,

$$\frac{\partial f}{\partial t} + \mathbf{v} \frac{\partial f}{\partial \mathbf{r}} - \frac{\partial \Phi}{\partial \mathbf{r}} \frac{\partial f}{\partial \mathbf{v}} = 0, \quad (1)$$

supplemented by the Poisson equation for the conjoint potential  $\Phi(\mathbf{r}, t)$  [Henon 1982; Binney & Tremaine 2008]. The definition of quasi-stationary state is often associated with the *virial equation*, which is valid for a set of  $N$  gravitating points in the center of mass coordinate system:

$$\frac{1}{2} \frac{d^2 J(t)}{dt^2} = 2K(t) + W(t), \quad (2)$$

where

$$\begin{aligned} J(t) &= \sum_1^N m_i \mathbf{r}_i^2, \\ K(t) &= \sum_1^N m_i \mathbf{v}_i^2 / 2, \quad \text{and} \\ W(t) &= -G \sum_{i=1}^{N-1} \sum_{j=i+1}^N \frac{m_i m_j}{|\mathbf{r}_i - \mathbf{r}_j|} \end{aligned} \quad (3)$$

are, respectively, the moment of inertia of the system, its kinetic and potential energies, whereas  $m_i$ ,  $\mathbf{r}_i(t)$  and  $\mathbf{v}_i(t)$  are the mass, radius-vector and the speed of the  $i$ -th star.<sup>1</sup> The total mass  $M = \sum m_i$  of the star system and its total energy  $E$  are assumed to be given. If the motions occur in a limited region of space, then, averaging Eq. (2) over time, we obtain the equality  $2\langle K \rangle + \langle W \rangle = 0$ , called the *virial theorem* (Landau & Lifshitz 1976). Stellar systems are not closed in space, but it is assumed that after some time a quasi-stationary state is reached, in which the left side of Eq. (2) becomes negligible, so, marking the parameters in

---

<sup>1</sup>The virial equation as presented here follows from Eq. (5.133) and the Lagrange-Jacobi identity (5.136) of Chandrasekhar (1942) monograph.

quasi-stationary state with asterisks, we can take

$$2K_* + W_* = 0. \quad (4)$$

Within the framework of the discussed here approach, one should understand the quasi-stationary state as the *virial equilibrium state* (VES). The characteristic time interval for reaching VES will be denoted as  $T_v$ . Some models of internal rearrangement of a system evolving from the virial to a true quasi-stationary equilibrium were studied by Levin, Pakter & Rizzato (2008) and Benetti et al. (2014).

Finally, the third stage, the relaxation of the system's core towards the Maxwell-Boltzmann state, takes even more time  $T_r$ . For half a century it was believed that this process is due solely to the *irregular* gravitational field of the system, which is defined as the difference between the real and smoothed fields (Ambartsumian 1938; Chandrasekhar 1942; Spitzer 1987). Since the spatial density of stars in galaxies is low, the main contribution to the process is made by pair collisions (close passages) of stars; it is taken into account by the non-zero *collisional term* on the right side of Eq. (1). An explicit representation of this term for systems with Coulomb or gravitational interaction was given by Landau (1937). Research in recent decades has associated relaxation to a more efficient process of *dynamic chaos* (Gurzadyan & Savvidy 1984, 1986); the corresponding relaxation time  $T_r \simeq N^{1/3}T_d$  (according to Rastorguev & Sementsov 2006, the exponent is 1/5). Thermodynamic equilibrium is never reached already due to the long-range nature of the gravitational force (Lynden-Bell 1967; Levin, Pakter & Rizzato 2008; Levin et al. 2014; Benetti et al. 2014); in addition, the uncloseness of the system is manifested in its external parts.

As regards the evolution at the second of the stages mentioned above, the nature of the observed fast "Maxwellization" of galaxies in a regular field remained unclear for a long time. The revival of research in this direction was initiated by Henon (1964) and Lynden-Bell (1967); the latter proposed an appropriate stochastic mechanism, as he called it, *violent relaxation*. In the current understanding, this implies the importance of collective processes in systems with long-range interaction (Shu 1978; Levin, Pakter & Rizzato 2008; Levin et al. 2013; Gurzadyan & Kocharyan 2009). On the other hand, numerical simulations, starting with van Albada (1982) studies and up to Halle, Colombi & Peirani (2019) and Sylos Labini & Capuzzo-Dolcetta (2020) recent calculations, gradually clarify the commensurate role of radial instabilities and internal density fluctuations that lead to the formation of local substructures of increasing size. Unlike  $T_d$  and  $T_r$ , no explicit representation of  $T_v$  in terms of the integral parameters of the system has been found so far,

especially since it depends on the initial state. Quantification is hindered by the extreme complexity of combining the kinetic and Poisson equations.

In this connection, the virial equation attracts more attention. It should be taken to a deeper level of description compared to the kinetic equation in one its form or another, because the latter is inevitably formulated with finite accuracy, while the virial equation is due only to the fundamental fact that the potential energy in the gravitational interaction of a pair of point-like bodies is inversely proportional to the distance between them, i.e., it is a *homogeneous function* of coordinates of degree  $-1$ . Among other things, the virial equation is valid for any, small or large, number of interacting points, while the accuracy of Eq. (1) drops as  $N$  decreases. For  $N \gg 1$ , the collisionless Boltzmann equation is consistent with the virial equation in the sense that Eq. (2), in its continuous version, can be derived from Eq. (1).

Since the total energy of an isolated system  $E = K(t) + W(t)$  is conserved in time, Eq. (2) is usually written as

$$\frac{1}{2} \frac{d^2 J(t)}{dt^2} = 2E - W(t). \quad (5)$$

For a gravitationally bound system, a necessary (but not sufficient) stability condition is  $E < 0$  (Chandrasekhar 1942); we will assume that this condition is satisfied. Equation (5) includes two unknown functions of time, and therefore, by itself, does not allow complete description of even the integral properties of the system. However, it can be hoped that it will provide some information about *the character* of evolution and the corresponding time intervals. The present paper is devoted to elucidating this possibility.

## 2 Signs of different evolution of two characteristic radii of the system

Usually the degree of proximity to the state of virial equilibrium is given by the value of the *virial ratio*

$$V(t) \equiv \frac{2K(t)}{|W(t)|} = 2 \left[ 1 - \frac{E}{W(t)} \right], \quad 0 \leq V < 2. \quad (6)$$

In view of Eq. (4), the values of the kinetic and potential energies in VES are

$$K_* = -E, \quad W_* = 2E, \quad (7)$$

so the equilibrium virial ratio  $V_* = 1$ . As the time scale in VES, we take  $T_* \equiv \mathfrak{R}_*/v_*$  – the time of intersection of the mean harmonic radius  $\mathfrak{R}_*$  of the system with the characteristic velocity  $v_*$ . The values of the last two follow from Eq. (7) and the definitions

$$K_* \equiv \frac{1}{2} M v_*^2, \quad W_* \equiv -\frac{GM^2}{2\mathfrak{R}_*}. \quad (8)$$

In this way we get:

$$v_* = \left( \frac{2|E|}{M} \right)^{1/2}, \quad \mathfrak{R}_* = \frac{GM^2}{4|E|}, \quad T_* = \frac{G}{4} \left( \frac{M^5}{2|E|^3} \right)^{1/2}. \quad (9)$$

The literature uses similar definitions with minor differences in numerical coefficients; the values adopted here are convenient for what follows. Notice that all these parameters are determined by the values of  $M$  and  $E$ . We can write the last of Eqs. (9) as  $T_* = (3/2\pi G\rho_*)^{1/2}$ , where characteristic density  $\rho_* \equiv 3M/4\pi\mathfrak{R}_*^3$ ; as expected, the time scale  $T_*$  turns out to be of the order of dynamic time  $T_d$ . Since the estimates of  $v_*$  and  $\mathfrak{R}_*$  can be found directly from observations, the first two of formulas (9) make it possible to estimate the total mass and energy of the system (Bahcall & Tremaine 1981; Binney & Tremaine 2008). The discussed picture of evolution is illustrated in Fig. 1 (see also Fig. 6.1 in Ciotti (2021) monograph).

It is convenient to pass in Eq. (5) to the searched quantities of a single physical nature – the root-mean-square radius  $R(t)$  and the mean harmonic radius  $\mathfrak{R}(t)$ , which are defined as follows:

$$R^2(t) \equiv \frac{1}{M} \sum_1^N m_i \mathbf{r}_i^2, \quad (10)$$

$$\mathfrak{R}^{-1}(t) \equiv \frac{2}{M^2} \sum_{i=1}^{N-1} \sum_{j=i+1}^N \frac{m_i m_j}{|\mathbf{r}_i - \mathbf{r}_j|},$$

so that

$$J(t) = MR^2(t), \quad W(t) = -\frac{GM^2}{2\mathfrak{R}(t)}, \quad (11)$$

and Eq. (5) takes the form:

$$\frac{d}{dt} \left( R \frac{dR}{dt} \right) = \frac{GM}{2\mathfrak{R}(t)} - \frac{2|E|}{M}. \quad (12)$$

Finally, introducing, with the help of Eq. (9), the dimensionless variables

$$\tau \equiv t/T_*, \quad x \equiv \mathfrak{R}/\mathfrak{R}_*, \quad \text{and} \quad y \equiv R/\mathfrak{R}_*, \quad (13)$$

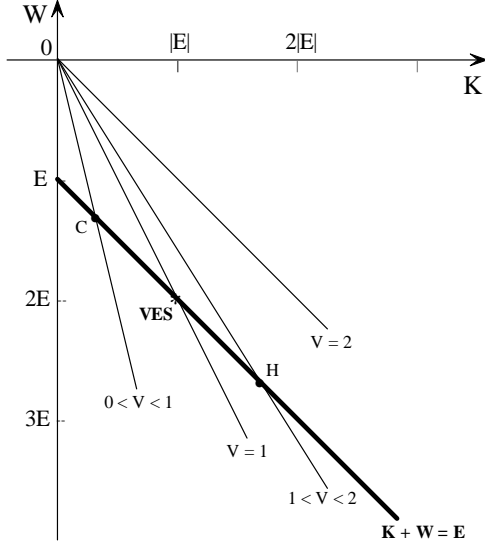


Figure 1: In the  $(K, W)$  plane, the system evolves along the straight line  $K(t) + W(t) = E$ , approaching on average a *virial equilibrium state* (VES). The thin lines correspond to fixed values of the virial ratio  $V$ . The letters  $C$  and  $H$  denote “cold” and “hot” configurations, which are characterized by the values  $K < |E|$  and  $K > |E|$ , respectively.

we reduce the virial equation to the dimensionless form with all unit coefficients:

$$\frac{d}{d\tau} \left( y \frac{dy}{d\tau} \right) = \frac{1}{x} - 1, \quad (14)$$

while the definition (6) for the virial ratio becomes

$$V(\tau) = 2 - x(\tau), \quad 0 < x(\tau) \leq 2. \quad (15)$$

We emphasize an important fact that has not been discussed before:

*The mean harmonic radius of a system with a negative total energy does not exceed twice the equilibrium value.*

The assertion follows from the definition  $\mathfrak{R}/\mathfrak{R}_* \equiv 2|E|/|W|$  and the inequalities  $K > 0$ ,  $|E| < |W|$ . A clear evidence is that the lines  $V = \text{const}$  in Fig. 1 do not intersect with the line corresponding to the given value  $E$  when  $\text{const} \geq 2$ .

In view of the above, the approximation to virial equilibrium over time means that the harmonic radius of the system  $\mathfrak{R}(t)$ , changing in a relatively narrow range

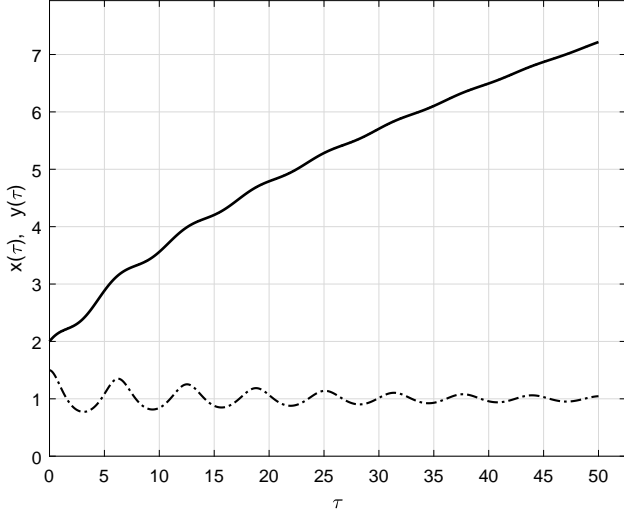


Figure 2: Change in the RMS radius of the system  $y(\tau)$  (solid line) for a given behavior of the harmonic radius  $x(\tau)$  (dash-dotted line).

of values  $(0, 2\mathfrak{R}_*)$ , tends to its equilibrium value (9), i.e.,  $x(\tau) \rightarrow 1$ , the second derivative of  $R^2(t)$  tends to zero, while the RMS radius  $R(t)$  tends to a finite or infinite value. To show the theoretical possibility of the described scenario, we, anticipating the discussion in the next section, present in Fig. 2 the evolution of the harmonic and root-mean-square radii for a given behavior of the first radius, while the change in the second radius is calculated according to the virial equation (14). Specifically, the initial values  $x(0) = 1.5$  and  $y(0) = 2.0$  were set, and it was assumed that  $x(\tau)$  tends to 1, experiencing an exponential decay and oscillations with a period  $2\pi T_*$  (see Eq. (23) below). Note that  $y^2(\tau)$  grows linearly as  $\tau \rightarrow \infty$ .

Supporting this model is the practical constancy of the half-mass radius  $R_h$  in time when calculating the evolution of isolated stellar systems (Spitzer 1987). Within the framework of King’s models, which describe well the internal structure of the globular clusters, the mean harmonic radius  $\mathfrak{R} \simeq 2.5R_h$  and, therefore, also changes little (private communication, A. Rastorguev, 2023).

Thus, the ratio of radii

$$q(\tau) \equiv \frac{R}{\mathfrak{R}} = \frac{y(\tau)}{x(\tau)} \quad (16)$$

can vary within wide limits. It is useful to estimate the parameter  $q$  for several continuous, for simplicity, density distributions that differ significantly from each other. Table 1 lists the corresponding data for systems with central symmetry.

Table 1: Characteristics of systems with central symmetry for various spatial density distributions  $\rho(r)$ . The following designations are accepted:  $\rho_0$  – central density;  $M$  – total mass;  $\bar{R}$ ,  $R$  and  $\mathfrak{R}$  – respectively, mean, mean square and mean harmonic radii.

No.	$\rho(r)/\rho_0$	$M/\rho_0 a^3$	$\bar{R}/a$	$R/a$	$\mathfrak{R}/a$	$q \equiv R/\mathfrak{R}$
1	$1, r \leq a; 0, r > a$	$4\pi/3$	$3/4$	$\sqrt{3/5}$	$5/6$	$2(3/5)^{3/2} \approx 0.9295$
2	$\exp(-r/a)$	$8\pi$	$3$	$2\sqrt{3}$	$16/5$	$5\sqrt{3}/8 \approx 1.0825$
3	$\exp(-r^2/a^2)$	$\pi^{3/2}$	$2/\sqrt{\pi}$	$\sqrt{3/2}$	$\sqrt{\pi/2}$	$\sqrt{3/\pi} \approx 0.9772$
4	$(1 + r^2/a^2)^{-5/2}$	$4\pi/3$	$2$	$\infty$	$16/3\pi$	$\infty$
5	$(1 + r^2/a^2)^{-2}$	$\pi^2$	$\infty$	$\infty$	$\pi$	$\infty$

These distributions can be conditionally considered as instantaneous (but not sequential) states of a star cluster evolving in accordance with the kinetic and Poisson equations. To calculate the values given in the table, note that for a continuous distribution, the mass  $M(r)$  inside a sphere of radius  $r$  and the potential energy  $W$  are defined by the formulas

$$M(r) = 4\pi \int_0^r \rho(r)r^2 dr, \quad (17)$$

$$W = -4\pi G \int_0^\infty \rho(r)M(r)r dr,$$

so the analogs of Eqs. (10) are reduced, using Eq. (11), to

$$R^2 = \frac{4\pi}{M} \int_0^\infty \rho(r)r^4 dr, \quad (18)$$

$$\mathfrak{R}^{-1} = \frac{8\pi}{M^2} \int_0^\infty \rho(r)M(r)r dr.$$

As Table 1 shows, for the first three, relatively homogeneous distributions, the values of  $q$  are close to 1. Apparently, these density distributions are adequate only at the initial stage of evolution. The values of  $q$  remain of the same order for fairly significant deviations from the spherical symmetry of the density distribution, for example, towards ellipsoidality. More important is the density distribution in the outer region of the system. The theoretical estimates by von Hoerner (1956), the thorough numerical modeling by van Albada (1982), reinforced by physical arguments of Trenti, Bertin & van Albada (2005), further simulations of cluster evolution by Yangurazova & Bisnovaty-Kogan (1984), Levin, Pakter



& Rizzato (2008), Levin et al. (2013), Joyce, Marcos & Sylos Labini (2010), Sylos Labini (2013), Halle, Colombi & Peirani (2019), and Sylos Labini & Capuzzo-Dolcetta (2020) indicate the formation of a power-law density distribution  $\rho(r) \propto r^{-\alpha}$  with exponent  $\alpha \sim 3.3-4$  in the halo. The last two examples of Table 1 are just that. Example No. 4 is the system of Schuster (1883) and Plummer (1911), which was repeatedly used in connection with studies of globular star clusters. With density distributions as flat as in Examples 4 and 5, the integrals for  $R$  diverge, so the  $q$ -factor is infinitely large.

The above models assume a more or less gradual change in density with distance from the center. An idea of the reverse behavior is given by a two-layer model with radii  $R_1, R_2$  and densities  $\rho_1, \rho_2$  in the central and outer zones, respectively. We do not present the corresponding formulas because of their cumbersomeness. The general conclusion is that at moderate values of the ratio  $\rho_1/\rho_2$ , the  $q$ -factor is still close to 1, and only when  $\rho_1/\rho_2 \gg 1$  and  $R_1/R_2 < 0.1$  can  $q$  more than 10 be achieved.

Thus, it seems likely that relatively homogeneous systems at the initial stage of evolution are characterized by  $q(\tau)$  of the order of 1, while the  $q$ -factor increases significantly in the course of further evolution as a dense core and extended halo of the system are formed.

### 3 Solutions for a given ratio of radii

In addition to the formal reason for the studying in Eq. (12) the dimensionless ratio of two unknown radii  $R(t)$  and  $\mathfrak{R}(t)$ , the function  $q(\tau)$  plays an important role by setting the systematic behavior of the RMS radius averaged over fast oscillations with a period of the order of dynamic time  $T_d$  (see Appendix).

In order to verify the oscillatory nature of the solutions of the virial equation, we write down Eq. (14) as

$$\frac{d}{d\tau} \left( y \frac{dy}{d\tau} \right) = \frac{q(\tau)}{y} - 1, \quad (19)$$

and assume first that the ratio of the radii does not change with time. Lynden-Bell (1967) additionally linearized the corresponding equation; Chandrasekhar & Elbert (1972) found a rather complicated analytical solution to a non-linear equation. Written in parametric form, the exact solution of Eq. (19) at  $q(\tau) \equiv q_0$

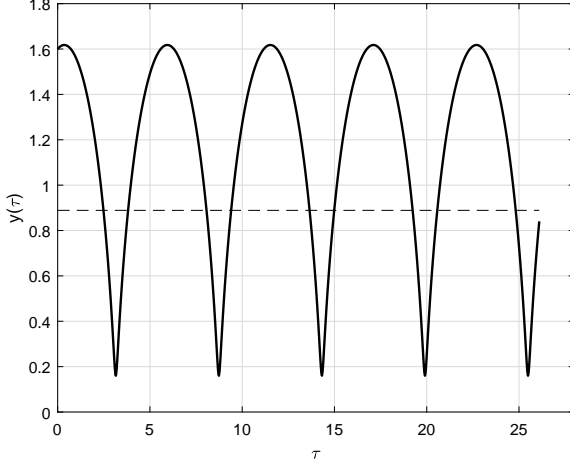


Figure 3: Changing the RMS radius  $y(\tau)$  in a model with constant ratio  $y/x \equiv q_0$  at initial values  $y_0 = 1.60$ ,  $y'_0 = 0.10$ ,  $V_0 = 0.20$ . The dashed line corresponds to  $q_0 = 8/9$ .

describes a classical cycloid

$$\begin{cases} y = q_0 - a \cos \theta - b \sin \theta, \\ \tau = q_0 \theta - a \sin \theta - b(1 - \cos \theta), \quad 0 \leq \theta < \infty, \end{cases} \quad (20)$$

whereas the mean harmonic radius of the system

$$x(\tau) = y(\tau)/q_0 = 1 - (a/q_0) \cos \theta - (b/q_0) \sin \theta \quad (21)$$

oscillates around the equilibrium value  $x_* = 1$ . The constants  $a$  and  $b$  are determined by the initial state:

$$a = q_0 - y_0, \quad b = -y_0 \cdot y'_0. \quad (22)$$

It is convenient to proceed from three initial values, namely, the pair  $(y_0, y'_0)$  and the virial ratio  $V_0$ ; then, according to Eqs. (15) and (16), we have  $x_0 = 2 - V_0$  and  $q_0 = y_0/x_0$ .

Equation (6) shows that values of the kinetic energy less or greater than  $|E|$  correspond to virial ratio values less or greater than 1 (see Fig. 1); how it is accepted, we call the respective states of the system “cold” and “hot”. The mean harmonic radius  $\mathfrak{R}$  of the former state exceeds the equilibrium value  $\mathfrak{R}_*$ , while  $\mathfrak{R} < \mathfrak{R}_*$  for the latter state.

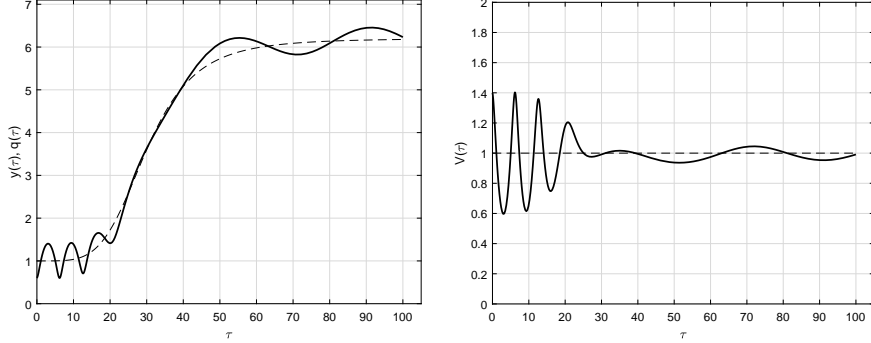


Figure 4: Solution of Eq. (19) with initial data  $V_0 = 1.40$ ,  $y_0 = 0.60$ ,  $y'_0 = 0.10$ . Left: RMS radius  $y(\tau)$  of the system (solid line) and  $q(\tau)$  function (dashed line). Right: Virial ratio  $V(\tau)$  (solid line) and unit level corresponding to VES (dashed line).

An example solution for  $V_0 = 0.20$  (“cold” system) is shown in Fig. 3. The period of oscillations of the cycloid in real time is equal to  $q_0 P_*$ , where

$$P_* = 2\pi T_* = \frac{\pi G}{2} \left( \frac{M^5}{2|E|^3} \right)^{1/2} = \sqrt{6\pi/G\rho_*}, \quad (23)$$

and  $\rho_* = 3M/4\pi\mathfrak{R}_*^3$  is the characteristic density of the cluster.

It is clear that the undamped, so-called homologous oscillations give only a preliminary description of the early evolution of a self-gravitating system. As noted at the end of the previous section, to estimate the characteristic time to reach virial equilibrium, it is necessary to take into account a progressive macroscopic inhomogeneity of the system. Accordingly, we must turn to a model with a time-varying ratio of radii  $R/\mathfrak{R}$ . The Appendix to this paper shows that the approximate solution of Eq. (19) with an arbitrary function  $q(\tau)$ , on which only the condition of its slow change on the time scale  $T_*$  is imposed, is a generalization of the classical cycloid, namely:

$$\begin{cases} y = u(\theta) - a(\theta) \cos \theta - b(\theta) \sin \theta, \\ \tau = \theta u(\theta) - a(\theta) \sin \theta - b(\theta)(1 - \cos \theta), \quad 0 \leq \theta < \infty. \end{cases} \quad (24)$$

Here, the base function  $u(\theta)$  is given by the implicit equation  $u = q(\theta \cdot u)$ , and the variable coefficients  $a(\theta)$  and  $b(\theta)$  depend on  $u(\theta)$ , that is, they are also given by the function  $q(\tau)$ . In the case of  $q(\tau) \equiv q_0$ , we get  $u = q_0$ , the coefficients  $a, b$  become constant, and we return to the model considered above. The physical meaning of representation (24) is that the functions  $u(\theta), a(\theta)$  and  $b(\theta)$  change,

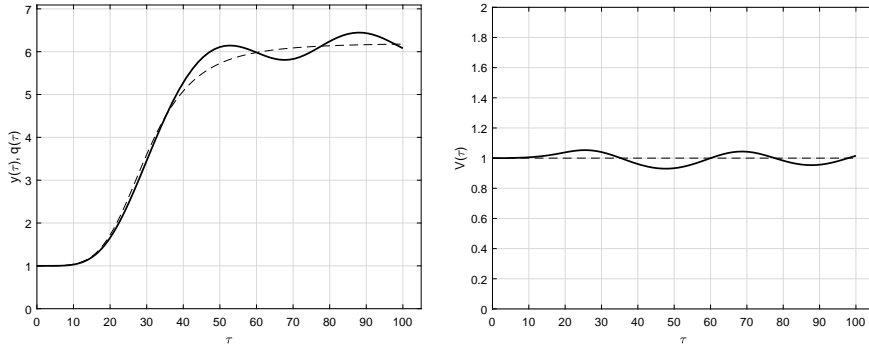


Figure 5: Solution of Eq. (19) with initial data  $V_0 = 1.0$ ,  $y_0 = 1.0$ ,  $y'_0 = 0$  corresponding to virial equilibrium state. Explanations are the same as in Fig. 4.

following  $q(\tau)$ , relatively slowly, while their trigonometric factors reflect precisely these rapid variations of the RMS radius around  $q(\tau)$ , and the mean harmonic radius and virial ratio – around the equilibrium value equal to 1. Our numerical examples show that in the immediate vicinity of the VES, the oscillation period slightly increases.

Not as informative as the analytical, but more accurate approach is the direct numerical solution of Eq. (19) for a given  $q(\tau)$ . Figure 4 gives an idea of a typical evolutionary pattern, in this case a “hot” system. The behavior of the mean harmonic radius  $x(\tau)$  is not shown because, in view of Eq. (15), it is a reflection of  $V(\tau)$  relative to the equilibrium level. We see several rapid initial fluctuations in both the RMS radius and the virial ratio, however, later  $y(\tau)$  follows the given function  $q(\tau)$ , while  $V(\tau)$  and  $x(\tau)$  practically stabilize around the equilibrium level  $x_* = 1$ . *This means that, over a period of two to three dozen of dynamic time intervals  $T_*$ , an equilibrium core with radius  $\mathfrak{R}_*$  is formed in the system, while the surrounding halo, which determines the RMS radius  $R(t)$ , continues to expand.*

The pattern of virial oscillations seen in the right Fig. 4 has the same character as that obtained by numerical simulation of the dynamics of a multiparticle system (see, for example, Fig. 6 in Trenti, Bertin & van Albada 2005). Fast oscillations are just a ringing against the backdrop of a slower reorganization of the system. Eventually, it is possible that after two dozen dynamic time periods  $T_*$  the harmonic radius of the system  $x(\tau)$  will become close to 1, and then, as the virial equation (14) shows, the further evolution of the root-mean-square radius of the system is described by simple law  $R(t)/\mathfrak{R}_* \simeq q(\tau) \simeq (c_1\tau + c_2)^{1/2}$ , where  $\tau = t/T_*$  and  $c_1, c_2$  are some dimensionless constants.

For control, one should also check the evolution of the system, which was initially in a virial equilibrium state. As can be seen in Fig. 5, the rapid oscillations of the radii and the virial ratio have disappeared, the RMS radius  $y(\tau)$  still follows  $q(\tau)$ , while the quasi-equilibrium nucleus experiences only long-term weak oscillations. This was to be expected.

The difference in the behavior of the system core and halo seems quite plausible, but we should not forget that in the context considered here it is partly determined by the specification of the  $q(\tau)$  function. This prompted us to consider models with different types of  $q(\tau)$ ; all cases, except for extremely "hot" systems, show the same behavior.

## 4 Concluding remarks

The above analysis supports two features of the evolution of a stellar system towards virial equilibrium. First, its integral characteristics fluctuate during two to three tens of dynamic time  $T_*$  until the virial ratio stabilizes near the equilibrium value  $V_* = 1$ . Secondly, the root-mean-square and mean harmonic radii vary in time in different ways, so the assumption previously accepted by a number of researchers about the approximate equality of radii is far from reality. As already noted, the first conclusion agrees with the results of numerical simulation of self-gravitating systems at  $N \gg 1$ . The second conclusion means a fundamentally different behavior of the moment of inertia of the system relative to the center of gravity and its potential energy.

Further details of the process of approaching the virial equilibrium state remain hidden when only the virial equation is analyzed. Additional data are desirable, at least in the form of approximate relationships between the integral characteristics of the system. On the other hand, the difference between evolutionary paths of the RMS and the mean harmonic radii can be easily elucidated on the basis of both already performed and future numerical simulations.

## Acknowledgements

The author is grateful to A.S. Rastorguev for useful comments.

## Data availability

No new data were generated or analysed in support of this research.

## Appendix. Approximate analytical solution of the virial equation

A nonlinear differential equation of the second order

$$y \left[ \frac{d}{d\tau} \left( y \frac{dy}{d\tau} \right) + 1 \right] = q(\tau) \quad (\text{A1})$$

is considered in the domain  $\tau \geq 0$  for a given non-negative function  $q(\tau)$ . The approach presented below, which goes back to the method of Van der Pol (1927), is widely used in the theory of oscillations.

We will look for a solution in a parametric form:

$$\begin{cases} y = u(\theta) - a(\theta) \cos \theta - b(\theta) \sin \theta, \\ \tau = \theta u(\theta) - a(\theta) \sin \theta - b(\theta)(1 - \cos \theta), \quad \theta \geq 0, \end{cases} \quad (\text{A2})$$

where  $u(\theta)$ ,  $a(\theta)$  and  $b(\theta)$  are some unknown functions slowly varying over an interval of length  $2\pi$ . In particular, they can be constant. Specifically, we assume that  $|u'(\theta)/u(\theta)| \ll 1$ , and similar inequalities hold for the coefficients  $a$  and  $b$ . Under this condition, the solution averaged over an interval of length  $2\pi$  is

$$\langle y(\theta) \rangle = \frac{1}{2\pi} \int_{\theta}^{\theta+2\pi} y(t) dt \simeq u(\theta), \quad (\text{A3})$$

which determines the physical meaning of the function  $u(\theta)$ .

We have from Eqs. (A2):

$$\begin{cases} dy/d\theta = u' - a' \cos \theta + a \sin \theta - b' \sin \theta - b \cos \theta, \\ d\tau/d\theta = u + \theta u' - a' \sin \theta - a \cos \theta - b'(1 - \cos \theta) - b \sin \theta. \end{cases} \quad (\text{A4})$$

According to the above condition, we can neglect here terms with derivatives, i.e. put

$$\begin{cases} u' - a' \cos \theta - b' \sin \theta = 0, \\ \theta u' - a' \sin \theta - b'(1 - \cos \theta) = 0, \end{cases} \quad (\text{A5})$$

so that Eqs. (A4) take the form:

$$\begin{cases} dy/d\theta = a \sin \theta - b \cos \theta, \\ d\tau/d\theta = u - a \cos \theta - b \sin \theta = y. \end{cases} \quad (\text{A6})$$

Dividing the top of Eqs. (A6) by the bottom gives:

$$y \frac{dy}{d\tau} = a \sin \theta - b \cos \theta. \quad (\text{A7})$$

Moreover, Eqs. (A6) shows that the derivatives with respect to  $\tau$  and with respect to  $\theta$  are connected by the relation

$$\frac{d}{d\tau} = \frac{1}{d\tau/d\theta} \cdot \frac{d}{d\theta} = \frac{1}{y} \frac{d}{d\theta}. \quad (\text{A8})$$

Applying this operator to Eq. (A7), taking into account the first of Eqs. (A2) and the condition of smallness of derivatives, we find:

$$\begin{aligned} y \frac{d}{d\tau} \left( y \frac{dy}{d\tau} \right) &= \frac{d}{d\theta} (a \sin \theta - b \cos \theta) \simeq \\ &a \cos \theta + b \sin \theta = u(\theta) - y. \end{aligned} \quad (\text{A9})$$

Thus,

$$y \left[ \frac{d}{d\tau} \left( y \frac{dy}{d\tau} \right) + 1 \right] = u(\theta), \quad (\text{A10})$$

which coincides with Eq. (A1) provided that

$$u(\theta) = q(\tau). \quad (\text{A11})$$

Here it suffices to restrict ourselves to the first term in the representation of  $\tau$  from Eqs. (A2), so that the function  $u(\theta)$  is found from the implicit equation

$$u = q(\theta \cdot u). \quad (\text{A12})$$

Finally, given the known function  $u(\theta)$ , one can find coefficients  $a(\theta)$  and  $b(\theta)$  by solving the system of linear Eqs. (A5) with respect to  $a'$  and  $b'$ , and then integrating the results. We will not go into further technical details.

## References

- [1] Ambartsumian V. A., 1938, Ann. Leningrad St. Univ., 22, 19. Transl. in: J. Goodman & P. Hut, eds., 1985, *The Evolution of Star Clusters: Dynamics of Star Clusters*, p. 521, Reidel, Boston.
- [2] Bahcall J., Tremaine S., 1981, ApJ, 244, 805.
- [3] Benetti F. P. C., Ribeiro-Teixeira A. C., Pakter R., Levin Y., 2014, Phys. Rev. Lett., 113, 100602.
- [4] Binney J., Tremaine S., 2008, *Galactic Dynamics*, Princeton Univ. Press, Princeton.
- [5] Chandrasekhar S., 1942, *Principles of Stellar Dynamics*, Chicago: Univ. of Chicago Press. Reissued by Dover 1960.
- [6] Chandrasekhar S., Elbert D.D., 1972, MNRAS, 155, 435.
- [7] Ciotti L., 2021, *Introduction to Stellar Dynamics*, Cambridge Univ. Press.
- [8] Gurzadyan V.G., Savvidy G.K., 1984, Doklady AN SSSR, 277, 69.
- [9] Gurzadyan V.G., Savvidy G.K., 1986, A&A, 160, 203.
- [10] Gurzadyan V.G., Kocharyan A.A., 2009, A&A, 505, 625.
- [11] Jeans J. H., 1915, MNRAS, 76, 71.
- [12] Jeans J. H., 1919, *Problems of Cosmogony and Stellar Dynamics*, Cambridge Univ. Press, Cambridge.
- [13] Joyce M., Marcos B., Sylos Labini F., 2010, arXiv:1011.0614 [astro-ph.CO].
- [14] Halle A., Colombi S., Peirani S., 2019, A&A 621, A8.
- [15] Henon M., 1964, Ann. d'Astrophys., 27, 83.
- [16] Henon M., 1982, A&A., 114, 211.
- [17] Hoerner S., von, 1957, ApJ, 125, 451.
- [18] Landau L. D., 1937, Journ. Exp. Theor. Phys. 7, 203.



- [19] Landau L. D., Lifshitz E. M., 1976, *Theoretical Physics. V. I, Mechanics*, 3rd ed., Elsevier.
- [20] Levin Y., Pakter R., Rizzato F. B., 2008, *Phys. Rev.*, E78, 021130.
- [21] Levin Y., Pakter R., Rizzato F. B., Teles T. N., Benetti F. P. C., 2014, *Phys. Rep.* 535, 1.
- [22] Lynden-Bell D., 1967, *MNRAS*, 136, 101.
- [23] Plummer H.C., 1911, *MNRAS*, 71, 460.
- [24] Rastorguev A.S., Sementsov V. N., 2006, *Astronomy Letters*, 32, 14.
- [25] Schuster A., 1883, *British Assoc. Report* 427.
- [26] Shu F. H., 1978, *ApJ*, 225, 83.
- [27] Spitzer L., Jr., 1987, *Dynamical Evolution of Globular Clusters*, Princeton Univ. Press, Princeton.
- [28] Sylos Labini F., 2013, *MNRAS*, 429, 679.
- [29] Sylos Labini F., Capuzzo-Dolcetta R., 2020, *A&A*, 643, A118.
- [30] Trenti M., Bertin G., & van Albada T.S., 2005, *A&A* 433, 57.
- [31] van Albada T.S., 1982, *MNRAS*, 201, 939.
- [32] Van der Pol B., 1927, *The London, Edinburgh and Dublin Phil. Mag. & J. of Sci.*, 2 (7), 978.
- [33] Yangurazova L.R., Bisnovaty-Kogan G.S., 1984, *Ap. & Sp. Sci.*, 100, 319.